

## Impacts of rainfall intensity and slope gradient on rill erosion processes at loessial hillslope

Haiou Shen<sup>a,b</sup>, Fenli Zheng<sup>a,b,\*</sup>, Leilei Wen<sup>a,b</sup>, Yong Han<sup>b,c</sup>, Wei Hu<sup>b,c</sup>

<sup>a</sup> College of Natural Resources and Environment, State Key Laboratory of Soil Erosion and Dryland Farming on the Loess Plateau, Northwest A & F University, Yangling, Shaanxi 712100, PR China

<sup>b</sup> Institute of Soil and Water Conservation, CAS & MWR, Yangling, Shaanxi 712100, PR China

<sup>c</sup> University of Chinese Academy of Sciences, Beijing 100049, PR China



### ARTICLE INFO

#### Article history:

Received 5 February 2015

Received in revised form 7 May 2015

Accepted 16 September 2015

#### Keywords:

Rill erosion

Rainfall intensity

Slope gradient

Flow hydraulic parameter

Hydrodynamic parameter

### ABSTRACT

Rill erosion constitutes one of the mechanisms of soil loss by water on agricultural land. However, studies on hillslope rill erosion characteristics and its intrinsic mechanisms are still unclear. The objectives of this study were to investigate the impacts of rainfall intensity and slope gradient on hillslope rill erosion processes, rill flow hydraulic characteristics and dynamic mechanisms. A soil pan (10 m long, 1.5 m wide and 0.5 m deep and with an adjustable slope gradient of 0–30°) was subjected to rainfall simulation experiments under three rainfall intensities (50, 75 and 100 mm h<sup>-1</sup>) of representative erosive rainfall and three typical slope gradients (10, 15 and 20°) on the Loess Plateau of China. The results showed that rill erosion exhibited significant contributions to hillslope soil erosion, occupying 62.2–84.8% of hillslope soil loss. The equation between the rill erosion rate with rainfall intensity and slope gradient was generated, which indicated that the impacts of rainfall intensity on hillslope rill erosion were greater than those of slope gradient. For the experimental treatments, the mean headward erosion rates varied between 2.2 and 8.2 cm min<sup>-1</sup>, and they increased with an increase in either rainfall intensity or slope gradient. Most rill flow belonged to turbulent and subcritical flow regimes. The critical shear stress, the critical stream power, and the critical unit stream power of rill occurrence were 0.986 Pa, 0.207 N m<sup>-1</sup> s<sup>-1</sup>, and 0.002 m s<sup>-1</sup>, respectively. Additionally, hillslope rill erosion was sensitive to rill flow velocity and stream power. In a word, rainfall intensity and slope gradient exhibited important impacts on rill erosion processes and its hydrodynamic characteristics. Therefore, preventing rainfall erosion and weakening slope gradient effects through conservation tillage are useful for reduction of rill erosion at loessial hillslopes.

© 2015 Elsevier B.V. All rights reserved.

### 1. Introduction

Rill erosion constitutes one of the mechanisms of soil loss by water on sloping croplands and rangelands in many areas around the world (Bewket and Sterk, 2003; Kimaro et al., 2008; Porto et al., 2014; Zheng and Tang, 1997). Agricultural productivity and environmental quality have deteriorated due to the increase in soil loss on hillslopes. Several studies (e.g., Bryan and Rockwell, 1998; Di Stefano et al., 2013) have noted that there is a marked increase in soil erosion rate coinciding with rill initiation. This increase is of obvious practical importance in soil conservation. Furthermore, rill development is also of geomorphic significance,

with potential implications for the hillslope and drainage network evolution (Bryan and Rockwell, 1998).

Rill erosion is most likely a major soil erosion pattern because, rill channels transport sediment particles both detached from the interrill areas and sourced from the rill wetted perimeter (Bewket and Sterk, 2003; Bruno et al., 2008; Nearing et al., 1997). Although the knowledge of rill erosion characteristics (Bryan and Rockwell, 1998; Wirtz et al., 2012) and its influencing factors (Berger et al., 2010; Römkens et al., 2001; Wei et al., 2007) has increased, the study of rill erosion processes is still a subject of unclear description and dependence. The reported estimates (e.g., Zheng and Tang, 1997) of rill erosion on the Loess Plateau of China are extremely worrisome. Thus, a deeper insight into rill erosion processes on hillslopes of this region is essential.

Many studies have reported that rill erosion is directly controlled by combined actions of runoff and soil (Sun et al.,

\* Corresponding author at: Institute of Soil and Water Conservation, No. 26, Xi'nong Road, Yangling, Shaanxi 712100, PR China. Fax: +86 29 87012210.

E-mail address: [fzh@ms.iwsc.ac.cn](mailto:fzh@ms.iwsc.ac.cn) (F. Zheng).

2013). Other factors may have indirect influences on rill erosion by increasing or decreasing the effects of direct factors (Wirtz et al., 2012). Rainfall intensity and slope gradient are two important influencing factors to rill erosion. Rill erosion usually increased with increasing rainfall intensity and slope gradient (Berger et al., 2010; Römkens et al., 2001). It is a general agreement that concentrated flow causes rill development (Romero et al., 2007), while raindrop impact play more significant roles in interrill erosion (Wirtz et al., 2012). On the Loess Plateau of China, rains with the features as high intensity, short duration and high frequency cause the greatest proportion of runoff and soil loss (Wei et al., 2007). Additionally, slope gradient is relatively steep and changes between 3 and 12° at the sheet erosion dominant zone and 12–25° at the rill erosion dominant zone (Zheng et al., 2005).

The intrinsic mechanisms of rill erosion are still unclear due to its complexity, especially under different physical processes (Wirtz et al., 2013). Rill erosion and development are linked to some hydraulic characteristics of channel flow, such as flow velocity, Reynolds number, Froude number, and Darcy–Weisbach resistance coefficient (An et al., 2012; Bryan and Rockwell, 1998; Reichert and Norton, 2013). Flow velocity has significant influence on magnitudes of runoff erosion and entrainment capacities (Li et al., 2006). Reynolds number is essentially a ratio of kinetic to viscous forces of flow. Froude number represents a ratio of kinetic to gravitational flow forces (Polyakov and Nearing, 2003). Then, Darcy–Weisbach resistance coefficient describes head loss due to fluid shear stress applied on the soil surface. Flow in rills is characterized by subcritical (Froude number <1) and supercritical (Froude number >1) flows, with transitional (Reynolds number = 1000–2000) and turbulent (Reynolds number >2000) flow regimes (Reichert and Norton, 2013).

It is important to evaluate the dynamic mechanisms of rill erosion because soil detachment and transport by flow are of processes of energy consumption. Shear stress, stream power, and unit stream power are basic hydrodynamic parameters (An et al., 2012). These parameters are commonly used to evaluate soil detachment rates and characterize critical dynamic conditions of soil erosion occurrence (e.g., Nearing et al., 1997; Reichert and Norton, 2013). Although studies on the dynamic mechanisms of soil erosion have been paid more attention, the hydrodynamic characteristics of rill erosion are still unclear.

Some researchers (e.g., Lei and Tang, 1998) suggest using Reynolds number as the criterion parameter of rill initiation. However, the results of Nearing et al. (1997) noted that Reynolds number was not a good predictor of rill flow hydraulic characteristics. Furthermore, Reichert and Norton (2013) noted that Darcy–Weisbach resistance coefficient seemed the best among the variables used to describe resistance to flow. Nearing et al. (1997) also reported that stream power was a consistent and appropriate predictor for unit sediment load. Thus, it is imperative to determine which parameters are optimal to characterize rill flow hydraulic characteristics and dynamic mechanisms of rill erosion.

Rainfall simulation is an ideal research method of rill erosion by replicating rill erosion processes and characteristics. An understanding of rill erosion processes is not only significant for the soil erosion prevention on sloping croplands but also of importance to soil erosion prediction models (Nearing et al., 1997; Sun et al., 2013). Therefore, a laboratory study was conducted under controlled experimental conditions. The objectives of this study are to investigate the impacts of rainfall intensity and slope gradient on rill erosion processes at the loessial hillslope, to study the rill headward erosion rate, analyze the rill flow hydraulic characteristics and dynamic mechanisms of rill erosion, and propose the most sensitive parameters for characterizing hillslope rill erosion.

## 2. Materials and methods

### 2.1. Experimental materials

The experiments were completed in the rainfall simulation laboratory of the State Key Laboratory of Soil Erosion and Dryland Farming on the Loess Plateau, Yangling City, China. The experiments were conducted in a slope adjustable pan 10 m long, 1.5 m wide and 0.5 m deep, with holes (2 cm aperture) at the bottom to facilitate drainage. The slope gradient ranged from 0 to 30° with adjustment intervals of 5°. In this study, three typical slope gradients of 10, 15 and 20° on the Loess Plateau of China were designed. A down sprinkler rainfall simulator system (Zheng and Zhao, 2004) was used to apply rainfall. This rainfall simulator including three nozzles can be set to any selected rainfall intensity ranging from 30 to 350 mm h<sup>-1</sup> by adjusting the nozzle size and water pressure. Three rainfall intensities (50, 75 and 100 mm h<sup>-1</sup>) of representative erosive rainfall on the Loess Plateau were applied to the soil pan. The fall height of the raindrops is 18 m above the ground, which allows all raindrops to reach terminal velocity prior to impact with the soil surface. Additionally, the simulated raindrop can successfully replicate the natural raindrop size and distribution (Shen et al., 2015).

The soil used in this study was the loessial soil, classified as a *Calcic Cambisols* (USDA Taxonomy), with 28.3% sand (>50 µm), 58.1% silt (50–2 µm), 13.6% clay content (<2 µm) and 5.9 g kg<sup>-1</sup> soil organic matter. The pipette method and the potassium dichromate oxidation-external heating method were used to analyze soil texture and soil organic matter, respectively. The tested soil was collected from 0 to 20 cm in the Ap horizon of a well-drained site in Ansai, Shaanxi Province, China. Impurities such as organic matter and gravels were removed from all the soil; though to keep its natural state, the soil was not passed through a sieve.

### 2.2. Preparation of the soil pan

Before packing the soil pan, the soil water content of the tested soil was determined and used to calculate how much soil was needed to pack the soil pan and obtain target bulk densities for different soil layers. First, a 5-cm-thick layer of sand was packed at the bottom of the soil pan, which allowed free drainage of excess water. Then, the layers over the sand layer were divided into a plow pan with a depth of 15 cm and a tilth layer with a depth of 20 cm to simulate local sloping croplands. The bulk densities for the plow pan and the tilth layer were 1.35 and 1.10 g cm<sup>-3</sup>, respectively. During the packing process, both the plow pan and the tilth layer were packed in 5-cm increments, and each packed soil layer was raked lightly before the next layer was packed to ensure uniformity and continuity in the soil structure. The soil amount of each layer was kept as constant as possible to maintain similar bulk density and uniform spatial distribution of soil particles. After completion of packing the soil pan, a manual tillage on the soil pan was performed at ~20 cm depth along the contour line, which is similar to the plowing depth of croplands. After plowing, the soil pan was allowed to settle for 48 h.

### 2.3. Experimental procedures

Before runs, the experimental soil pan was subjected to a pre-rain with the 30 mm h<sup>-1</sup> rainfall intensity until surface flow occurred. The duration of this pre-rain was ~25 min. The average soil water content before each rainfall was 23.4 ± 0.5% for all treatments. The purposes of the pre-rain were to maintain consistent soil moisture, consolidate loose soil particles by rainfall wetting, and reduce the spatial variability of surface conditions. The soil surface was covered with a plastic sheet after the pre-rain

to prevent soil moisture evaporation and surface sealing, and allowed to stand for 24 h.

Prior to running experiments, rainfall intensity was calibrated to confirm the run-rainfall intensity reaching the target rainfall intensity and meeting experimental requirements; uniformity was >90%. A total rainfall of 50 mm during each treatment for three designed rainfall intensities was maintained. Thus, rainfall durations were 60 min for 50 mm h<sup>-1</sup>, 40 min for 75 mm h<sup>-1</sup> and 30 min for 100 mm h<sup>-1</sup>. Each treatment was conducted two times.

After each treatment, the preparation for consecutive runs included drying, replacing top layer of soil and material lost from the prior experiment with the new loessial soil, breaking up clods, and smoothing out irregularities on the surface (Polyakov and Nearing, 2003).

#### 2.4. Experimental measurements

##### 2.4.1. Runoff and soil loss

One day after the pre-rain, the designed rainfall intensity (50, 75 or 100 mm h<sup>-1</sup>) was applied to the soil pan. For each treatment, runoff samples were collected in 15-L buckets as runoff occurred. The samples were measured in 1 or 2 min intervals for the whole rainfall durations, with 30 min for 100 mm h<sup>-1</sup>, 40 min for 75 mm h<sup>-1</sup> and 60 min for 50 mm h<sup>-1</sup>, respectively. These samples were weighed and then oven-dried at 105 °C to calculate sediment yield.

##### 2.4.2. Flow velocity and depth

Flow velocity and depth both on interrill and in rills were measured at five slope sections (1, 3, 5, 7 and 9 m) along the soil pan at 3 or 5 min intervals during rainfall processes. The KMnO<sub>4</sub> dye tracer method was used to measure flow velocity. The mass concentration of KMnO<sub>4</sub> liquid was 0.8%. The tracer movement time at the marked distance (0.5 m) was determined based on the color-front propagation using a stop-watch. Additionally, flow depth was measured perpendicularly using a thin ruler and read to 0.1-mm precision.

##### 2.4.3. Rill development

Manual measurements of each rill's width, depth and locations (*x,y*) along with rainfall duration, were performed when rills were generated. To aid in recognizing these rills, photographs were taken of the soil pan surface in 1 or 2 min intervals throughout each rain. After the completion of each rain, rill width and depth measurements were conducted along each rill channel at intervals of 5 or 10 cm. Furthermore, these measurements were also performed once sudden changes in the rill pattern occurred (Øygarden, 2003). The measurements were used to calculate rill volumes, which in turn, to estimate the magnitude of rill erosion.

#### 2.5. Data analysis

The statistical analysis was performed using SPSS 19.0 software (SPSS Inc., Chicago, IL, USA). Analysis of variance (ANOVA) was conducted to examine significant differences in runoff, soil loss rate, rill erosion rate, headward erosion rate, and hydraulic parameters among treatments of three rainfall intensities or three slope gradients. The values presented in this study were the mean with standard deviations. For the results of multiple comparisons, the method of least significant difference (LSD) procedure was used at the 95% confidence level. A correlation matrix of the Pearson correlation coefficient was used to analyze correlations of rill erosion per unit width, and rill flow hydraulic and hydrodynamic parameters.

A non-linear fitting method was applied to fit equations of soil loss, rill erosion, and critical runoff rate per unit width of rill occurrence by Matlab 7.9.0 software (MathWorks Inc., Massachusetts, USA). During the specific implementation process, the trust region method was applied, and the physical meaning of the equations considered.

Rill flow velocity (*V*), Reynolds number (*Re*), Froude number (*Fr*) and Darcy–Weisbach resistance coefficient (*f*) were calculated and used to analyze rill flow hydraulic characteristics. Furthermore, shear stress ( $\tau$ ), stream power ( $\omega$ ), and unit stream power ( $\varphi$ ) were selected to analyze the dynamic mechanisms of rill erosion. The calculation formulae of above parameters can be found in An et al. (2012).

### 3. Results

#### 3.1. Soil loss and rill erosion

There were no significant differences in runoff among treatments (Table 1). However, soil loss rates between treatments were of greater differences, especially for treatments of three rainfall intensities. Additionally, when slope gradient was increased from 10 to 15°, soil loss rates greatly increased. But there were no significant differences between slope gradients of 15 and 20°. The changing trend in rill erosion rates was similar to that in soil loss rates. Rill erosion rates accounted for 62.2–84.8% of soil loss rates for all treatments, and the average contribution was 73.4%.

The maximum rill erosion rate reached  $25.2 \pm 2.3 \text{ kg m}^{-2} \text{ h}^{-1}$  for the 100 mm h<sup>-1</sup> rainfall intensity with the slope gradient of 20° treatment (Table 1). The value was above 5.0 times greater than the minimum value for the 50 mm h<sup>-1</sup> rainfall intensity with the slope gradient of 10° treatment. When rainfall intensity was increased from 50 to 75 mm h<sup>-1</sup> and then increased from 75 to 100 mm h<sup>-1</sup>, rill erosion rates increased by 56.3–79.2% and 35.5–65.1%,

**Table 1**

Runoff, soil loss and rill erosion rates for different rainfall intensities and slope gradients.

Slope gradient (°)	Rainfall intensity (mm h <sup>-1</sup> )	Runoff (mm)	Soil loss rate (kg m <sup>-2</sup> h <sup>-1</sup> )	Rill erosion rate (kg m <sup>-2</sup> h <sup>-1</sup> )
10	50	$43.4 \pm 1.0 \text{ a}$	$7.4 \pm 0.8 \text{ b}$	$4.8 \pm 0.8 \text{ b}$
	75	$43.2 \pm 3.2 \text{ a}$	$11.5 \pm 1.8 \text{ ab}$	$8.6 \pm 1.4 \text{ ab}$
	100	$42.4 \pm 3.0 \text{ a}$	$17.0 \pm 3.4 \text{ a}$	$14.2 \pm 3.0 \text{ a}$
15	50	$43.8 \pm 1.3 \text{ a}$	$13.2 \pm 0.4 \text{ c}$	$8.4 \pm 0.1 \text{ b}$
	75	$45.0 \pm 2.1 \text{ a}$	$21.8 \pm 1.7 \text{ b}$	$13.5 \pm 1.8 \text{ ab}$
	100	$44.6 \pm 2.6 \text{ a}$	$31.6 \pm 3.0 \text{ a}$	$20.9 \pm 3.6 \text{ a}$
20	50	$41.5 \pm 1.2 \text{ a}$	$14.4 \pm 1.4 \text{ c}$	$11.9 \pm 1.5 \text{ b}$
	75	$43.3 \pm 0.6 \text{ a}$	$21.9 \pm 2.3 \text{ b}$	$18.6 \pm 2.8 \text{ ab}$
	100	$41.5 \pm 0.9 \text{ a}$	$32.2 \pm 1.8 \text{ a}$	$25.2 \pm 2.3 \text{ a}$

Values for different rainfall intensity treatments with the same slope gradient followed by different letters (a, b and c) are significantly different at  $p < 0.05$  according to the LSD test. The same in Tables 2 and 3.

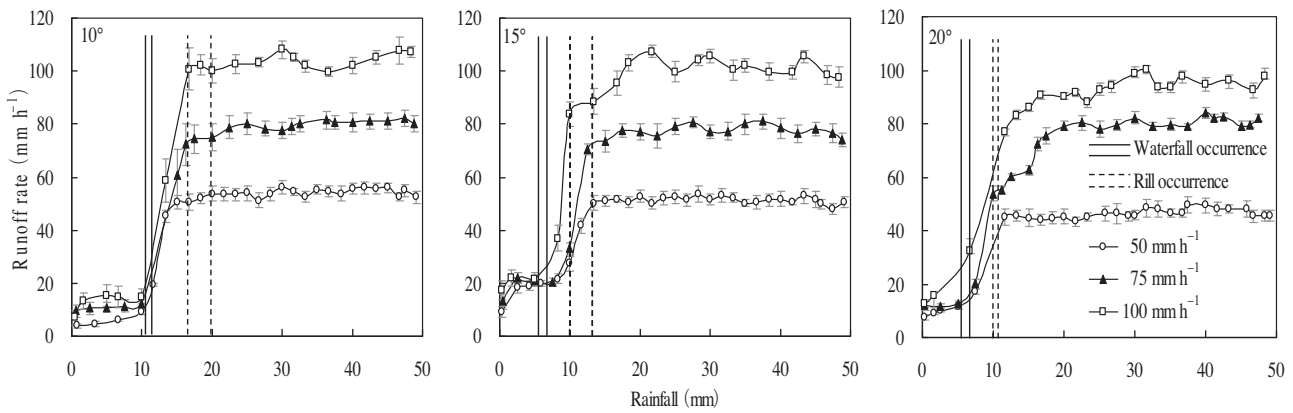


**Fig. 1.** Runoff rates versus rainfall for three rainfall intensities with three slope gradients. Error bars show the standard derivation among the repetitions ( $n=2$ ).

respectively. Then, rill erosion rates increased by 47.2–75.0% and 20.8–41.7%, respectively, as slope gradient was increased from 10 to 15° and then increased from 15 to 20°.

The soil loss and rill erosion equations with the optimal fit, based on an adjusted rainfall intensity factor and slope gradient factor, were established as follows:

$$SL = 0.010R^{1.230}S^{0.815} \quad (R^2 = 0.95, n = 18) \quad (1)$$

$$RE = 0.005R^{1.244}S^{0.940} \quad (R^2 = 0.96, n = 18) \quad (2)$$

where SL is soil loss rate ( $\text{kg m}^{-2} \text{h}^{-1}$ ); RE is rill erosion rate ( $\text{kg m}^{-2} \text{h}^{-1}$ ); R is rainfall intensity ( $\text{mm h}^{-1}$ ); and S is slope gradient ( $^\circ$ ).

According to Eqs. (1) and (2), both soil loss and rill erosion rates increased by power function with an increase in either rainfall intensity or slope gradient. The exponents of rainfall intensity in Eqs. (1) and (2) were relatively close, which were 1.230 and 1.244, respectively. Compared with the exponents of rainfall intensity, those of slope gradient were lower. They were 0.815 and 0.940 to the soil loss rate and the rill erosion rate, respectively. While the exponent of slope gradient in Eq. (1) was lower than that in Eq. (2).

### 3.2. Runoff and soil loss processes

#### 3.2.1. Runoff processes

The changing trends in runoff rates for all treatments were extremely similar (Fig. 1), which could obviously be divided into

three stages, that is, the initial stage, the rapid increasing stage and the relatively stable stage. Generally, the initial stage of runoff rates occurred before the rainfall amount reaching 10 mm. The rapid increasing stage of runoff rates happened before the rainfall amount reaching 20 mm. Then the relatively stable stage of runoff rates occurred after the rainfall amount reaching 20 mm.

The critical runoff rate per unit width of rill occurrence equation with the optimal fit, based on an adjusted rainfall intensity factor and slope gradient factor, was established as follows:

$$Q_c = 3.298R^{0.894}S^{-0.489} \quad (R^2 = 0.99, n = 18) \quad (3)$$

where  $Q_c$  is critical runoff rate per unit width of rill occurrence ( $\text{mm h}^{-1} \text{m}^{-1}$ ).

According to Eq. (3), the exponents of rainfall intensity and slope gradient to the critical runoff rates per unit width of rill occurrence were 0.894 and -0.489, respectively.

#### 3.2.2. Sediment processes

The changing trends in sediment concentration were similar to the changes of runoff rates, and could also be divided into three stages. Sediment concentration was lower in the initial stage, especially for the treatments of three rainfall intensities with the 10° slope gradient, whose values were  $<30 \text{ g L}^{-1}$  (Fig. 2). Moreover, an increase in slope gradient caused initial sediment concentration to increase significantly, and even the first peak value to occur.

The relatively stable stage of sediment concentration (Fig. 2) was a little different from that of runoff rates (Fig. 1), especially for greater rainfall intensity ( $100 \text{ mm h}^{-1}$ ) and greater slope gradient

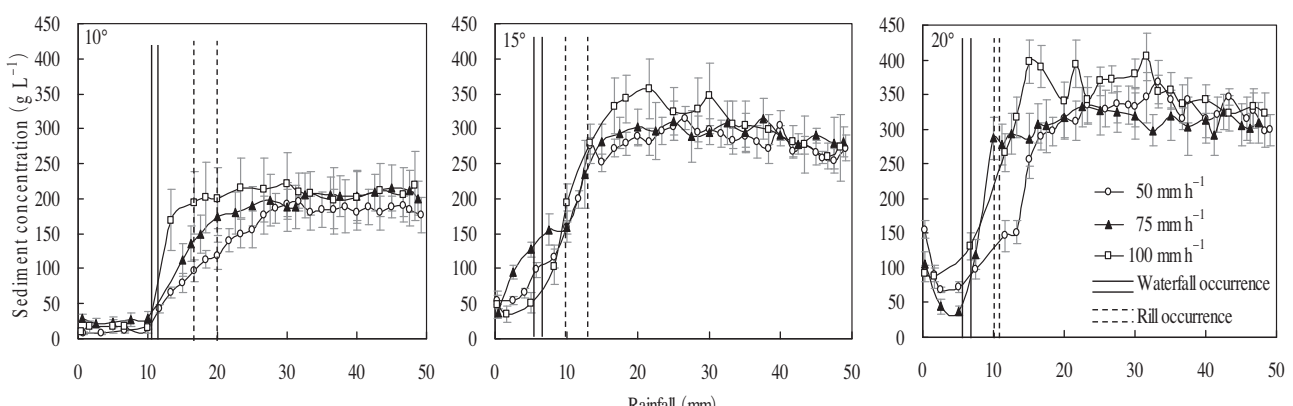


**Fig. 2.** Sediment concentration versus rainfall for three rainfall intensities with three slope gradients. Error bars show the standard derivation among the repetitions ( $n=2$ ).

**Table 2**

Rill headward erosion rates for different rainfall intensities and slope gradients.

Slope gradient ( $^{\circ}$ )	Rainfall intensity ( $\text{mm h}^{-1}$ )	Rill headward erosion rate ( $\text{cm min}^{-1}$ )	
		Max	Mean
10	50	5.9 $\pm$ 1.3 a	2.2 $\pm$ 0.3 b
	75	7.6 $\pm$ 1.4 a	3.6 $\pm$ 0.5 b
	100	8.7 $\pm$ 1.3 a	5.2 $\pm$ 0.5 a
15	50	6.4 $\pm$ 1.0 b	3.0 $\pm$ 0.3 c
	75	9.1 $\pm$ 1.1 ab	5.0 $\pm$ 0.6 b
	100	11.9 $\pm$ 2.1 a	6.9 $\pm$ 0.5 a
20	50	11.2 $\pm$ 1.1 a	3.8 $\pm$ 0.4 c
	75	11.3 $\pm$ 1.2 a	6.1 $\pm$ 0.6 b
	100	12.5 $\pm$ 1.6 a	8.2 $\pm$ 0.4 a

(15 or 20°) treatments. That is, sediment concentration firstly fluctuated at a relatively stable value, and then decreased with increasing rainfall. In this study, stable sediment concentration was ~4–12 times greater than initial sediment concentration.

### 3.3. Headward erosion rate

Both maximum and mean headward erosion rates increased with increasing rainfall intensity and slope gradient (Table 2). The maximum headward erosion rates even reached  $12.5 \pm 1.6 \text{ cm min}^{-1}$  for the  $100 \text{ mm h}^{-1}$  rainfall intensity with the 10° slope gradient treatment. Furthermore, mean headward erosion rates varied from 2.2 to  $8.2 \text{ cm min}^{-1}$ . There were major differences in the mean headward erosion rates among three rainfall intensities, but few differences among three slope gradients. When rainfall intensity was increased from 50 to  $75 \text{ mm h}^{-1}$  and then increased from 75 to  $100 \text{ mm h}^{-1}$ , the mean headward erosion rates increased by 61.3–68.6% and 34.9–44.6%, respectively. Additionally, the mean values of headward erosion rates increased by 32.2–38.2% and 18.3–26.7%, respectively, as slope gradient was increased from 10 to 15° and then increased from 15 to 20°.

### 3.4. Rill flow hydraulic characteristics and dynamic mechanisms of rill erosion

#### 3.4.1. Rill flow hydraulic characteristics

Mean rill flow velocity ( $V$ ) and Reynolds number ( $Re$ ) varied from  $20.6$  to  $24.6 \text{ cm s}^{-1}$  and  $1894.6$ – $3119.1$ , respectively, and they generally increased with an increase in either rainfall intensity or slope gradient (Table 3). There were significant differences in the

$Re$  values among treatments of three rainfall intensities, but relatively minor differences among treatments of three slope gradients. When rainfall intensity was increased from 50 to  $75 \text{ mm h}^{-1}$  and then increased from 75 to  $100 \text{ mm h}^{-1}$ , the values of  $Re$  increased by 20.3–35.9% and 14.4–28.0%, respectively. The increasing rates of  $Re$  were significantly higher than those as slope gradient was increased from 10 to 15° and then increased from 15 to 20°. With regards to Froude number ( $Fr$ ), the values ranged between 0.66 and 0.73. Furthermore, there were minor differences in the  $Fr$  values among treatments of three rainfall intensities or three slope gradients.

Darcy–Weisbach resistance coefficient ( $f$ ) varied from 3.19 to 6.52 (Table 3). For the 10 and 15° slope gradients treatments,  $f$  decreased with an increase in rainfall intensity. For the 20° slope gradient treatments, there were no significant differences in  $f$  among three rainfall intensities. However, the  $f$  values increased with an increase in slope gradient. There were significant differences in the  $f$  values among treatments of three slope gradients. When slope gradient was increased from 10 to 15° and then increased from 15 to 20°, the values of  $f$  increased by 50.6–55.5% and 18.9–28.6%, respectively. The above increasing rates were significantly higher than the decrease rates of  $f$  as rainfall intensity was increased from 50 to  $75 \text{ mm h}^{-1}$  and then increased from 75 to  $100 \text{ mm h}^{-1}$ .

#### 3.4.2. Dynamic mechanisms of rill erosion

Average shear stress ( $\tau$ ), stream power ( $\omega$ ) and unit stream power ( $\varphi$ ), ranging from  $1.837$  to  $3.784 \text{ Pa}$ ,  $0.379$ – $0.932 \text{ N m}^{-1} \text{ s}^{-1}$  and  $0.036$ – $0.090 \text{ m s}^{-1}$ , respectively, increased with increasing

**Table 3**

Rill flow hydraulic parameters for different rainfall intensities and slope gradients.

Slope gradient ( $^{\circ}$ )	Rainfall intensity ( $\text{mm h}^{-1}$ )	$V (\text{cm s}^{-1})$	$Re$	$Fr$	$f$
10	50	$20.6 \pm 1.5$ b	$1894.6 \pm 93.1$ c	$0.66 \pm 0.03$ a	$3.56 \pm 0.35$ a
	75	$22.0 \pm 2.0$ ab	$2311.3 \pm 226.5$ b	$0.67 \pm 0.05$ a	$3.30 \pm 0.48$ ab
	100	$23.7 \pm 1.6$ a	$2704.3 \pm 173.7$ a	$0.69 \pm 0.03$ a	$3.19 \pm 0.42$ b
15	50	$21.9 \pm 1.6$ b	$1930.1 \pm 97.6$ c	$0.69 \pm 0.02$ a	$5.36 \pm 0.17$ a
	75	$23.1 \pm 2.3$ ab	$2322.1 \pm 257.3$ b	$0.71 \pm 0.06$ a	$5.13 \pm 0.64$ ab
	100	$24.3 \pm 2.7$ a	$2971.4 \pm 325.5$ a	$0.71 \pm 0.09$ a	$4.85 \pm 0.61$ b
20	50	$22.3 \pm 1.3$ b	$2005.9 \pm 199.0$ c	$0.71 \pm 0.05$ a	$6.52 \pm 0.57$ a
	75	$24.0 \pm 2.7$ a	$2726.6 \pm 385.6$ b	$0.73 \pm 0.08$ a	$6.10 \pm 0.86$ a
	100	$24.6 \pm 2.2$ a	$3119.1 \pm 292.4$ a	$0.70 \pm 0.07$ a	$6.24 \pm 0.79$ a

$V$ : mean rill flow velocity;  $Re$ : Reynolds number;  $Fr$ : Froude number;  $f$ : Darcy–Weisbach resistance coefficient.

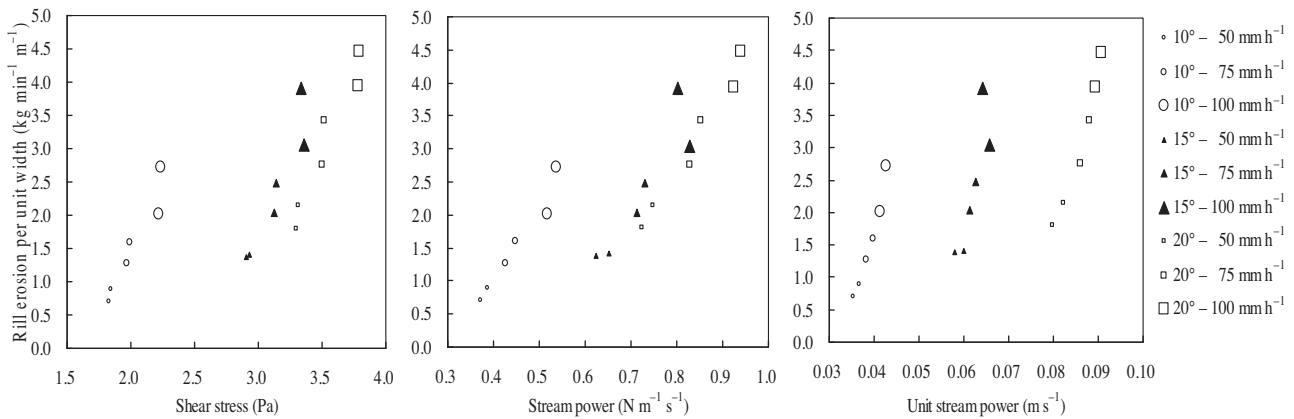


**Fig. 3.** The relationships between rill erosion per unit width and shear stress, stream power, unit stream power for different rainfall intensities and slope gradients.

either rainfall intensity or slope gradient (Fig. 3). Rill erosion per unit width significantly increased with increases in  $\tau$ ,  $\omega$ , and  $\varphi$ .

The relations between rill erosion per unit width and above three hydrodynamic parameters were described well by the linear function. For all treatments, the linear relations can be expressed as:

$$\left\{ \begin{array}{l} D_r = 1.225 (\tau - 0.986) \quad (R^2 = 0.59, n = 18) \\ D_r = 5.046 (\omega - 0.207) \quad (R^2 = 0.72, n = 18) \\ D_r = 38.723 (\varphi - 0.002) \quad (R^2 = 0.50, n = 18) \end{array} \right. \quad (4)$$

where  $D_r$  is rill erosion per unit width ( $\text{kg min}^{-1} \text{m}^{-1}$ );  $\tau$  is shear stress (Pa);  $\omega$  is stream power ( $\text{N m}^{-1} \text{s}^{-1}$ ); and  $\varphi$  is unit stream power ( $\text{m s}^{-1}$ ).

The critical force could be obtained by above relations. When no rill erosion occurred, i.e.,  $D_r=0$ , then the critical hydrodynamic force was determined. The critical shear stress, the critical stream power, and the critical unit stream power computed by the Eq. (4) were 0.986 Pa, 0.207  $\text{N m}^{-1} \text{s}^{-1}$ , and 0.002  $\text{m s}^{-1}$ , respectively.

#### 3.4.3. Correlations of rill erosion and flow hydraulic and hydrodynamic parameters

There were stronger correlations between rill erosion per unit width ( $D_r$ ) and other hydraulic and hydrodynamic parameters, whose correlation coefficients decreased in the order of  $V > Re > \omega > \tau > f > Fr > f$  (Table 4).

With regards to the rill flow hydraulic parameters, the strongest correlations were  $V$  with the other parameters, which were followed in descending order by  $Fr$ ,  $Re$  and  $f$ . For the hydrodynamic parameters, the strongest correlations were  $\omega$  with the other two parameters, which were followed by  $\tau$  and  $\varphi$ .

**Table 4**

Correlation matrix for rill erosion per unit width and rill flow hydraulic and hydrodynamic parameters.

	$D_r$	$V$	$Re$	$Fr$	$f$	$\tau$	$\omega$	$\varphi$
$D_r$	1	0.927**	0.907**	0.618**	0.481*	0.767**	0.847**	0.708**
$V$	0.927**	1	0.926**	0.694**	0.347	0.685**	0.782**	0.604**
$Re$	0.907**	0.926**	1	0.433	0.150	0.510*	0.631**	0.439
$Fr$	0.618**	0.694**	0.433	1	0.624**	0.755**	0.770**	0.744**
$f$	0.481*	0.347	0.150	0.624**	1	0.905**	0.839**	0.942**
$\tau$	0.767**	0.685**	0.510*	0.755**	0.905**	1	0.988**	0.954**
$\omega$	0.847**	0.782**	0.631**	0.770**	0.839**	0.988**	1	0.936**
$\varphi$	0.708**	0.604**	0.439	0.744**	0.942**	0.954**	0.936**	1

$n = 18$ . \* $p < 0.05$ , \*\* $p < 0.01$ .  $D_r$ : rill erosion per unit width;  $V$ : mean rill flow velocity;  $Re$ : Reynolds number;  $Fr$ : Froude number;  $f$ : Darcy–Weisbach resistance coefficient;  $\tau$ : shear stress;  $\omega$ : stream power;  $\varphi$ : unit stream power.

## 4. Discussion

### 4.1. Hillslope rill erosion characteristics

Runoff was similar in all treatments because the same pre-rain, and the same total rainfall of 50 mm applied by controlling rainfall duration (60 min for 50  $\text{mm h}^{-1}$ , 40 min for 75  $\text{mm h}^{-1}$  and 30 min for 100  $\text{mm h}^{-1}$ ) for each treatment. Compared with runoff, there were greater differences in soil loss rates among treatments (Table 1). Soil detachment occurred by several processes, predominant of which were hydraulic forces of raindrop impact and flow in rills (Polyakov and Nearing, 2003). With increasing rainfall intensity and slope gradient, both rainfall erosivity and runoff erosivity on the hillslope increased (Table 3). Thus, soil loss rates increased correspondingly.

The occupying percent of rill erosion rate to soil loss rate was quite high. This result was similar to that investigated by Zheng et al. (1987), who noted that rill erosion contributed 74.2% to hillslope soil loss. Therefore, carrying out studies of rill erosion has important impacts on soil erosion prevention and control because rill erosion exhibited significant contributions to hillslope soil erosion.

The designed rainfall intensities and slope gradients caused major differences in rill erosion (Table 1). Additionally, the increments of rill erosion rates were different with increasing rainfall intensity and slope gradient. The reason was that there were critical values of influencing rill erosion (Léonard and Richard, 2004). If rainfall intensity or slope gradient was increased and close to the influencing critical values, the increments of rill erosion rates would relatively slow down.

According to Eqs. (1) and (2), the impacts of rainfall intensity on hillslope soil erosion and rill erosion were similar. However, the impacts of slope gradient on rill erosion were greater than those on hillslope soil erosion. Furthermore, rainfall intensity exhibited greater impacts on hillslope soil erosion and rill erosion than slope gradient. This was consistent with the results by Berger et al. (2010). Therefore, taking effective measures to protect the soil by weakening rainfall erosion, such as wheat straw mulch (Zhang et al., 2009) and a temporary grass ley (Fullen, 1998), is useful for soil conservation.

### 4.2. Hillslope rill erosion processes

There were lower runoff rates in the initial stage (Fig. 1). The reason was that soil surface sealing had not formed and raindrop

splash erosion was dominant in the initial stage of rainfall. Therefore, soil infiltration rates were greater and runoff rates were lower than those in the other two stages. With the formation of soil surface sealing and surface flow, interrill erosion evolved into the dominant soil erosion pattern. Then, soil infiltration rates decreased and runoff rates increased correspondingly in the rapid increasing stage. The confluence of surface flow on the interrill erosion areas prepared hydrodynamic conditions for rill development (Bruno et al., 2008). With the rainfall, surface flow gradually converted into concentrated flow, which was the main cause of rill erosion (Owoputi and Stolte, 1995). In the concentrated flow path, runoff erosivity increased enough to scour soil clods. This resulted in the occurrence of small waterfalls (Shen et al., 2015). Then, small waterfalls evolved into rill headcuts, and rills occurred correspondingly. As rill erosion occurred and evolved into the dominant erosion pattern, runoff rates rapidly increased to the relatively stable stage.

Although total runoff was similar for all treatments (Table 1), runoff rates, especially for stable runoff rates, were significantly different (Fig. 1). An increase in rainfall intensity or slope gradient induced greater runoff rates accompanying with stronger fluctuations in runoff with rainfall. As mentioned above, the reason was due to the impacts of increases in rainfall erosivity and runoff erosivity on the hillslope.

According to Eq. (3), the critical runoff rate per unit width of rill occurrence increased with an increase in rainfall intensity, but decreased with an increase in slope gradient. The reason was that there was the same bearing rain area for treatments of the same slope gradient. Therefore, the critical runoff rate per unit width of rill occurrence increased with increasing rainfall intensity. However, the bearing rain area decreased with increasing slope gradient for treatments of the same rainfall intensity. This caused the critical runoff rate per unit width of rill occurrence to decrease. Additionally, rainfall intensity exhibited greater impacts on the critical runoff rate per unit width than slope gradient. Therefore, studies on the impacts of rainfall intensity on hillslope rill erosion are imperative in future.

Sediment concentration is an important parameter used to analyze hillslope soil detachment and transport processes. Detached loose soil particles caused by raindrop impacts were abundant on the hillslope at the beginning of the experiment, leading to relatively greater sediment concentration (Parsons and Stone, 2006; Wirtz et al., 2012). Additionally, the loss of detached loose soil particles at the beginning of the rainfall greatly increased with an increase in slope gradient (Fig. 2).

Small waterfalls generally occurred in the initial stage (Fig. 2), and the occurrence of small waterfalls was usually as a symbol of rill erosion appearing (He et al., 2013; Zheng and Tang, 1997). Thus, the interval between the occurrence of small waterfalls and rills could be as a judgment standard of difficulty or facility of rill erosion (He et al., 2013). Generally, an increase in rainfall intensity or slope gradient caused rill erosion more easily to occur under the experimental conditions.

In the rapid increasing stage, the increasing rates of sediment concentration became greater with an increase in rainfall intensity or slope gradient (Fig. 2). Generally, sediment transport capacity is a function of the flow's hydraulic forces and the transportability of sediment (Polyakov and Nearing, 2003). In this stage, soil detachment rates were lower or close to sediment transport capacity because interrill erosion was dominant on the hillslope.

Fluctuations in sediment concentration might be more strongly influenced by sediment transport capacity limitations rather than soil detachment (Nearing et al., 1997). In most cases, soil detachment rates were close to sediment transport capacity and, in some cases, sediment transport capacity was even exceeded. This was due to the occurrence of different hillslope

rill erosion phenomena (e.g., detachment, headward erosion, side-wall collapse, and undercut erosion) (Wirtz et al., 2012).

There was a marked increase in soil loss rate coinciding with rill initiation (Fig. 2). This was consistent with previous studies (e.g., Bryan and Rockwell, 1998; Di Stefano et al., 2013). The primary reason was that soil erodibility and sediment transport capacity by concentrated flow in rills were much greater than those caused by raindrop impact and overland flow (Auerswald et al., 2009). The another reason was due to flow in rills could transport both interrill eroded sediments and sediment particles eventually detached from the rill wetted perimeter once rills formed and developed (Bruno et al., 2008).

Headward erosion rates in hillslope rill erosion processes closely connected with soil loss (Han et al., 2002). Although there was certain randomness and chance in maximum headward erosion rates, the occurrence of these maximum values also had definite inevitability because it was a characterization of extreme changes of runoff erosivity. Mean headward erosion rates could more objectively reflect the status of rills' retreating than the maximum headward erosion rates.

The impacts of rainfall intensity on headward erosion were greater than those of slope gradient (Table 2). This could be explained that rainfall intensity exhibited greater impacts on rill dynamics (Fig. 3) and soil loss than slope gradient (Berger et al., 2010). Furthermore, the changing trends in mean headward erosion rates among rainfall intensities and slope gradients coincided with the changes of rill erosion rates (Table 1). The reason was also due to the critical values of influencing rill erosion (Léonard and Richard, 2004), if rainfall intensity or slope gradient was increased and close to the influencing critical values, the increment of headward erosion rates would relatively slow down.

#### 4.3. Hydraulic and dynamic mechanisms of rill erosion

It is a general agreement that rills are developed by concentrated flow (Romero et al., 2007; Wirtz et al., 2012). Therefore, the analysis of hydraulic parameters of concentrated flow in rills is necessary to characterize hillslope rill erosion mechanisms. Rainfall intensity and slope gradient exhibited similar reflection on mean rill flow velocity ( $V$ ) (Table 3). The values of Reynolds number ( $Re$ ) observed in all treatments were within the range reported for rills by Nearing et al. (1997). Flow in rills was characterized with transitional ( $Re = 1000–2000$ ) and turbulent ( $Re > 2000$ ) flow regimes (Reichert and Norton, 2013). For the 10 and 15° slope gradients with the 50 mm h<sup>-1</sup> rainfall intensity treatments,  $Re$  was within 1000–2000. Therefore, rill flow belonged to transitional flow. Then with regards to the remaining treatments in this study, rill flow belonged to turbulent flow. Furthermore, rainfall intensity exhibited greater impacts on  $Re$  than slope gradient. If rainfall intensity was increased and close to the influencing critical value, the increasing rate of  $Re$  would relatively slow down. This could be used to explain the results about changes of the rill erosion rates in Table 1 and the mean headward erosion rates in Table 2.

Froude number ( $Fr$ ) was also within the range reported for rills by Nearing et al. (1997) and Polyakov and Nearing (2003). The  $Fr$  values observed in this study were all  $<1$ . Therefore, rill flow belonged to subcritical flow (Reichert and Norton, 2013). Furthermore, minor differences in the  $Fr$  values among treatments illustrated that changes of rainfall intensity or slope gradient were not sensitive to  $Fr$ .

The changes of Darcy–Weisbach resistance coefficient ( $f$ ) versus rainfall intensity were consistent with the results of previous studies (e.g., Xiao et al., 2009). Once slope gradients were close to the critical value, the impact of rainfall intensity on  $f$  would weaken. Furthermore, the changes of the  $f$  values versus slope

gradient were consistent with the results of Zhang (1998), who noted that when slope gradients were  $>10^\circ$  at the loessial hillslope,  $f$  increased with an increase in  $Re$ . Additionally, the increments of the  $f$  values indicated that slope gradient exhibited greater impacts on  $f$  than rainfall intensity.

Soil particle detachment and transport are an energy consuming process (An et al., 2012). Therefore, studies on the dynamic mechanisms of rill erosion are useful (Fig. 3). Notably, the impacts of rainfall intensity on hydrodynamic characteristics of rill erosion were greater than the impacts of slope gradient. This also could be used to explain the results about changes of the rill erosion rates in Table 1 and the mean headward erosion rates in Table 2.

Correlations of rill erosion and flow hydraulic and hydrodynamic parameters indicated that the rill flow hydraulic and hydrodynamic parameters used in this study were suitable for characterizing the rill erosion mechanisms. Additionally, rill flow velocity was the most sensitive hydraulic parameter (An et al., 2012) to estimate rill flow hydraulic characteristics. Furthermore, stream power was the optimal hydrodynamic parameter (Nearing et al., 1997; Reichert and Norton, 2013) to characterize the dynamic mechanisms of rill erosion.

## 5. Conclusions

Rainfall simulation experiments focusing on rill erosion under three rainfall intensities (50, 75 and 100 mm h $^{-1}$ ) and three slope gradients (10, 15 and 20°) were conducted to investigate hillslope rill erosion processes, rill flow hydraulic characteristics and rill erosion dynamic mechanisms. The results showed that rill erosion on average occupied 73.4% of soil loss, which indicated that rill erosion exhibited significant contributions to hillslope soil erosion on the Chinese Loess Plateau. Generally, an increase in rainfall intensity or slope gradient caused rill erosion more easily to occur. The impacts of rainfall intensity on both hillslope soil erosion and rill erosion were greater than those of slope gradient. The mean headward erosion rates varying between 2.2 and 8.2 cm min $^{-1}$  increased with an increase in rainfall intensity or slope gradient. Most rill flow belonged to turbulent and subcritical flow regimes. The relations between rill erosion per unit width and shear stress, stream power, unit stream power were established, which indicated that the critical shear stress, the critical stream power, and the critical unit stream power were 0.986 Pa, 0.207 N m $^{-1}$  s $^{-1}$ , and 0.002 m s $^{-1}$ , respectively. Rill flow velocity was the optimal flow hydraulic parameter and stream power was the optimal hydrodynamic parameter to characterize the rill erosion mechanisms. In conclusion, there were important impacts of rainfall intensity and slope gradient on rill erosion processes and its hydrodynamic characteristics. Therefore, combating rainfall erosion and weakening slope gradient effects through conservation tillage are useful for rill erosion prevention and control.

## Acknowledgements

The work described in this paper was supported by the National Natural Science Foundation of China (grant no. 41271299) and the Non-profit Industry Financial Program of Ministry of Water Resources of China (grant no. 201201083). The authors would like to thank the editors and anonymous reviewers for their valuable comments and suggestions, which greatly improved our paper.

## References

- An, J., Zheng, F.L., Lu, J., Li, G.F., 2012. Investigating the role of raindrop impact on hydrodynamic mechanism of soil erosion under simulated rainfall conditions. *Soil Sci.* 177, 517–526.
- Auerswald, K., Fiener, P., Dikau, R., 2009. Rates of sheet and rill erosion in Germany—a meta-analysis. *Geomorphology* 111, 182–193.
- Berger, C., Schulze, M., Rieke-Zapp, D., Schlunegger, F., 2010. Rill development and soil erosion: a laboratory study of slope and rainfall intensity. *Earth Surf. Process. Landf.* 35, 1456–1467.
- Bewket, W., Sterk, G., 2003. Assessment of soil erosion in cultivated fields using a survey methodology for rills in the Chemoga watershed, Ethiopia. *Agric. Ecosyst. Environ.* 97, 81–93.
- Bruno, C., Di Stefano, C., Ferro, V., 2008. Field investigation on rilling in the experimental Sparacia area, South Italy. *Earth Surf. Process. Landf.* 33, 263–279.
- Bryan, R.B., Rockwell, D.L., 1998. Water table control on rill initiation and implications for erosional response. *Geomorphology* 23, 151–169.
- Di Stefano, C., Ferro, V., Pampalone, V., Sanzone, F., 2013. Field investigation of rill and ephemeral gully erosion in the Sparacia experimental area, South Italy. *Catena* 101, 226–234.
- Fullen, M.A., 1998. Effects of grass ley set-aside on runoff, erosion and organic matter levels in sandy soils in east Shropshire, UK. *Soil Tillage Res.* 46, 41–49.
- Han, P., Ni, J.R., Li, T.H., 2002. Headcut and bank landslip in rill evolution. *J. Basic Sci. Eng.* 10 (2), 115–125 (in Chinese, with English Abstract).
- He, J.J., Lu, Y., Gong, H.L., Cai, Q.G., 2013. Experimental study on rill erosion characteristics and its runoff and sediment yield process. *J. Hydraul. Eng.* 44 (4), 398–405 (in Chinese, with English Abstract).
- Kimaro, D.N., Poesen, J., Msanya, B.M., Deckers, J.A., 2008. Magnitude of soil erosion on the northern slope of the Uluguru Mountains, Tanzania: interrill and rill erosion. *Catena* 75, 38–44.
- Lei, A.L., Tang, K.L., 1998. Kinetic condition of rill erosion on loess sloping face. *J. Soil Eros. Soil Water Conserv.* 4 (3), 39–43 (in Chinese, with English Abstract).
- Léonard, J., Richard, G., 2004. Estimation of runoff critical shear stress for soil erosion from soil shear strength. *Catena* 57, 233–249.
- Li, P., Li, Z.B., Zheng, L.Y., 2006. Hydrodynamics process of soil erosion and sediment yield by runoff on loess slope. *Adv. Water Sci.* 17 (4), 444–449 (in Chinese, with English Abstract).
- Nearing, M.A., Norton, L.D., Bulgakov, D.A., Larionov, G.A., West, L.T., Dontsova, K.M., 1997. Hydraulics and erosion in eroding rills. *Water Resour. Res.* 33, 865–876.
- Owoputi, L.O., Stolte, W.J., 1995. Soil detachment in the physically based soil erosion process: a review. *Trans. ASAE* 38, 1099–1110.
- Øygarden, L., 2003. Rill and gully development during an extreme winter runoff event in Norway. *Catena* 50, 217–242.
- Parsons, A.J., Stone, P.M., 2006. Effects of intra-storm variations in rainfall intensity on interrill runoff and erosion. *Catena* 67, 68–78.
- Polyakov, V.O., Nearing, M.A., 2003. Sediment transport in rill flow under deposition and detachment conditions. *Catena* 51, 33–43.
- Porto, P., Walling, D.E., Capra, A., 2014. Using  $^{137}\text{Cs}$  and  $^{210}\text{Pb}_{\text{ex}}$  measurements and conventional surveys to investigate the relative contributions of interrill/rill and gully erosion to soil loss from a small cultivated catchment in Sicily. *Soil Tillage Res.* 135, 18–27.
- Reichert, J.M., Norton, L.D., 2013. Rill and interrill erodibility and sediment characteristics of clayey Australian Vertosols and a Ferrosol. *Soil Res.* 51, 1–9.
- Romero, C.C., Stroosnijder, L., Baigorria, G.A., 2007. Interrill and rill erodibility in the northern Andean Highlands. *Catena* 70, 105–113.
- Römkens, M.J.M., Helming, K., Prasad, S.N., 2001. Soil erosion under different rainfall intensities, surface roughness, and soil water regimes. *Catena* 46, 103–123.
- Shen, H.O., Zheng, F.L., Wen, L.L., Lu, J., Jiang, Y.L., 2015. An experimental study of rill erosion and morphology. *Geomorphology* 231, 193–201.
- Sun, L.Y., Fang, H.Y., Qi, D.L., Li, J.L., Cai, Q.G., 2013. A review on rill erosion process and its influencing factors. *Chin. Geogr. Sci.* 23, 389–402.
- Wei, W., Chen, L.D., Fu, B.J., Huang, Z.L., Wu, D.P., Gui, L.D., 2007. The effect of land uses and rainfall regimes on runoff and soil erosion in the semi-arid loess hilly area, China. *J. Hydrol.* 335, 247–258.
- Wirtz, S., Seeger, M., Ries, J.B., 2012. Field experiments for understanding and quantification of rill erosion processes. *Catena* 91, 21–34.
- Wirtz, S., Seeger, M., Zell, A., Wagner, C., Wagner, J.F., Ries, J.B., 2013. Applicability of different hydraulic parameters to describe soil detachment in eroding rills. *PLoS One* 8 (5), e64861.
- Xiao, P.Q., Zheng, F.L., Yao, W.Y., 2009. Flow pattern and hydraulic parameter characteristics in hillslope-gullyslope system. *Adv. Water Sci.* 20 (2), 236–240 (in Chinese, with English Abstract).
- Zhang, K.L., 1998. Study of flow resistance law in rill erosion on loess slope. *Yellow River* 20 (8), 13–15 (in Chinese, with English Abstract).
- Zhang, S.L., Lövdahl, L., Grip, H., Tong, Y.A., Yang, X.Y., Wang, Q.J., 2009. Effects of mulching and catch cropping on soil temperature, soil moisture and wheat yield on the Loess Plateau of China. *Soil Tillage Res.* 102, 78–86.
- Zheng, F.L., Tang, K.L., 1997. Rill erosion process on steep slope land of the Loess Plateau. *Int. J. Sediment. Res.* 12, 52–59.
- Zheng, F.L., Zhao, J., 2004. A brief introduction on the rainfall simulation laboratory and equipment. *Res. Soil Water Conserv.* 11 (4), 177–178 (in Chinese).
- Zheng, F.L., Tang, K.L., Zhou, P.H., 1987. Approach to the genesis and development of rill erosion on slope land and the way to control. *J. Soil Water Conserv.* 1 (1), 36–48 (in Chinese, with English Abstract).
- Zheng, F.L., He, X.B., Gao, X.T., Zhang, C.E., Tang, K.L., 2005. Effects of erosion patterns on nutrient loss following deforestation on the Loess Plateau of China. *Agric. Ecosyst. Environ.* 108, 85–97.